Su Hwan Kim[1]*
Sae Mi Hwang[2]*
Jong Min Lee[1]
Jin Hyun Kang[2]
Il Yup Chung[2]**
Bong Geun Chung[1]

[1]Department of Bionano Engineering, Hanyang University, Ansan, Korea
[2]Division of Molecular and Life Science, Hanyang University, Ansan, Korea

Received July 18, 2012
Revised August 28, 2012
Accepted October 5, 2012

Research Article

Epithelial-to-mesenchymal transition of human lung alveolar epithelial cells in a microfluidic gradient device

Epithelial-to-mesenchymal transition (EMT), a process in which epithelial cells undergo phenotypic transitions to fibrotic cells, is induced by stimulants including transforming growth factor-beta1 (TGF-β1). In the present study, we developed a microfluidic gradient device to reproduce EMT in A549 human lung alveolar epithelial cells in response to TGF-β1 gradients. The device was directly mounted on the cells that had grown in cell culture plates and produced a stable concentration gradient of TGF-β1 with negligible shear stress, thereby providing a favorable environment for the anchorage-dependent cells. A549 cells elongated with the characteristic spindle-shaped morphological changes with upregulation of alpha-smooth muscle actin, a mesenchyme marker, in a gradient-dependent manner, suggestive of EMT progression. We observed that at higher TGF-β1 concentrations ranging from 5 to 10 ng/mL, the cultures in the microfluidic device allowed to quantitatively pick up subtle differences in the EMT cellular response as compared with plate cultures. These results suggest that the microfluidic gradient device would accurately determine the optimal concentrations of TGF-β1, given that epithelial cells of different tissue origins greatly vary their responses to TGF-β1. Therefore, this microfluidic device could be a powerful tool to monitor EMT induced by a variety of environmental stresses including cigarette smoke with high sensitivity.

Keywords:
Epithelial-to-mesenchymal transition / Lung alveolar epithelial cells / Microfluidics
DOI 10.1002/elps.201200386

1 Introduction

Epithelial cells undergo phenotypic switching to mesenchymal cells in response to stress or injury through a process termed "epithelial-to-mesenchymal transition (EMT)" [1]. EMT is characterized by loss of polarity, cytoskeletal reorganization, and transition to a spindle-shaped morphology. The dramatic changes in cellular phenotype are accompanied by various molecular changes including loss of epithelial markers zonular occludens-1 and E-cadherin concomitant with acquisition of mesenchymal markers α-smooth muscle actin (α-SMA) and vimentin [2]. In particular, loss of E-cadherin is a universal feature of EMT, regardless of initiating stimuli [3]. Knockdown of E-cadherin expression by small inhibitory RNA can trigger EMT in the absence of exogenous stimulation [4, 5], while constitutive expression of E-cadherin provokes reversal of the mesenchymal phenotype [6]. EMT has previously been recognized to play an important role in regulating cellular differentiation not only during development and carcinogenesis but also during normal repair and scar formation following injury in adult tissues including the lungs, kidneys, and eyes [7]. In the lungs, EMT is believed to contribute significantly to lung fibrosis in response to drug- and airborne particle-induced injury [8].

EMT could be induced by a number of extracellular mediators individually or in combination, including transforming growth factor-beta1 (TGF-β1), fibroblast growth factor-2, epidermal growth factor (EGF), connective tissue growth factor, insulin-like growth factor, interleukin-1, hepatocyte growth factor, Wnt ligands [2], and environmental agents, notably cigarette smoke [9]. Among these, TGF-β1 served as a "master switch" in the induction of EMT and has been shown to mediate EMT in a variety of epithelial cell types of different tissue origins including lung. In this regard, TGF-β1 induced human and rat alveolar type II epithelial cells to undergo EMT, as evidenced by changes in the expression of biochemical markers of epithelial and mesenchymal cells [10, 11]. Alveolar epithelial type II cells served as progenitors

Correspondence: Professor Bong Geun Chung, Department of Bionano Engineering, Hanyang University, Ansan, Korea
E-mail: bchung@hanyang.ac.kr

Abbreviations: EGF, epidermal growth factor; **EMT**, epithelial-to-mesenchymal transition; **α-SMA**, α-smooth muscle actin; **TGF-β1**, transforming growth factor-beta1

*These authors contributed equally to this work.
**Additional corresponding author: Professor Il Yup Chung, E-mail: iychu@hanyang.ac.kr

Colour Online: See the article online to view Figs. 1 and 4 in colour.

for repair of the alveolar epithelium. Furthermore, several in vivo studies have demonstrated that TGF-β1 expression was increased at the active region of fibrotic change in idiopathic pulmonary fibrosis patients and bleomycin-treated animals [8, 12]. Thus, in vivo and in vitro evidence highlighted the importance of TGF-β1 as a most prevalent inducer of EMT of lung alveolar epithelial cells and intervention designed to inhibit EMT could lead to reduction in fibrosis of injured lung. However, the regulatory mechanism controlling EMT remains not completely understood.

Microfluidic gradient devices have been developed to study biological and pathological processes [13–15]. To investigate cellular behavior in response to gradient profiles in a microfluidic device, various approaches (e.g. chemical diffusion, electric field, shear stress, and extracellular matrix gradient) have been developed for applications of the chemotaxis [16–23], electrotaxis [24, 25], mechanotaxis [26, 27], and haptotaxis [28, 29]. In particular, molecular gradients played important roles in regulating protein expression. For example, a microfluidic gradient device has been used to investigate Wnt3a regulation of canonical β-catenin signaling [30]. When A375 melanoma cells containing Wnt/β-catenin reporters with pBARVS Venus expression were exposed to Wnt3a concentration gradients in the microfluidic device, the β-catenin activity was proportional to the gradient profile of Wnt3a. This microfluidic gradient device enabled the control of dynamic β-catenin pathway using the BARVS reporter gene in a real-time manner.

Lung epithelial cells exhibit different cellular responses depending on signaling molecules. Airway epithelial cells produce mucin proteins in response to EGF, while alveolar epithelial cells undergo EMT in response to TGF-β1. We have recently developed a microfluidic gradient device in which lung airway epithelial cells expressed a mucin protein in response to EGF [31]. In the device, various gradient profiles (e.g. nonlinear, linear, and flat gradients) were created with respect to the distance from the inlet microchannels and the mucin protein in the lung epithelial cells exposed to the flat gradient was highly expressed as compared with that in cells exposed to nonlinear and linear gradient profiles. It demonstrated that EGF gradient profiles enabled the control of mucin protein expression. This device was a useful tool to study the regulation of mucin expression in lung epithelial cells in response to diverse gradient profiles of a growth factor. However, the microfluidic gradient-based EMT studies have not yet been undertaken. Here, we investigate the effects of TGF-β1 gradients on the EMT response of human lung alveolar epithelial cells in the microfluidic device.

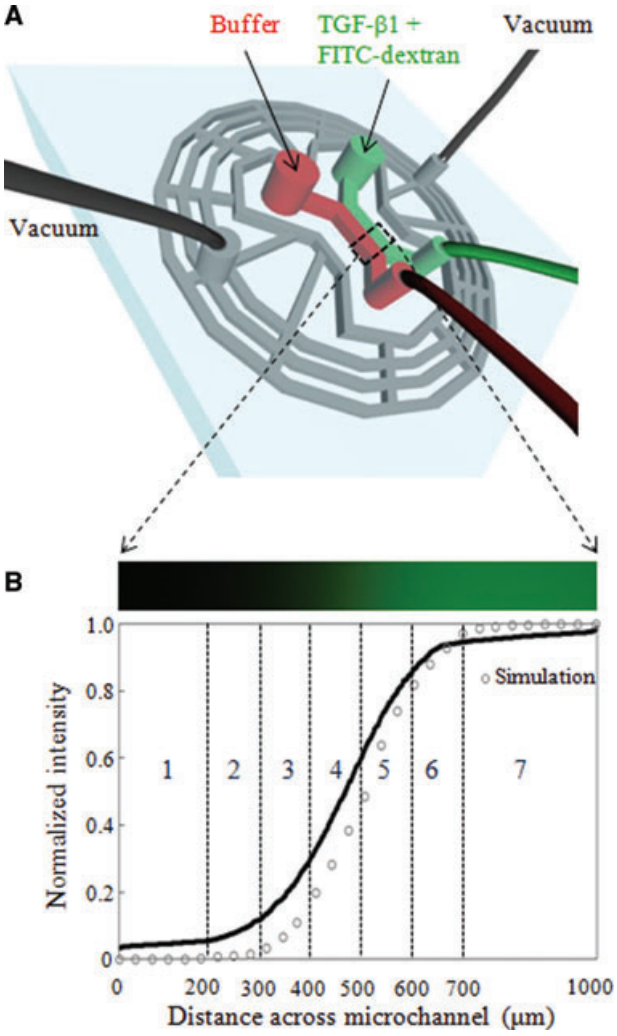

Figure 1. The microfluidic gradient device. (A) Schematic diagram of the microfluidic gradient device containing fluidic and vacuum network microchannels. (B) Experimental analysis and numerical simulation of the concentration gradient profiles in the microfluidic gradient device.

2 Materials and methods

2.1 Fabrication of the microfluidic gradient device

To fabricate the microfluidic gradient device with 100 μm thickness (Fig. 1A), a photomask thin film was designed by printing micropatterns on transparency films at 20 000 dots per inch (NEPCO, Korea). SU-8 negative photoresist (Microchem, MA, USA) was spin coated on a silicon wafer at 500 rpm for 10 s and 1000 rpm for 60 s. The wafer was baked at 65°C for 10 min and 95°C for 30 min on a hot plate. The photoresist layer was exposed to UV light for 60 s through the photomask thin film. The wafer was then postbaked at 65°C for 3 min and 95°C for 10 min. The photoresist-patterned wafer was subsequently micromolded using a PDMS elastomer and curing reagent (10:1 mixture), as previously described [31–33].

2.2 Characterization of gradient profiles and imaging analysis

To characterize the concentration gradient profiles in the microfluidic device, the buffer solution and FITC-dextran

(Sigma, USA) was withdrawn from the left and right inlet reservoirs of the microchannel using a syringe pump with a 0.15 μL/min flow rate (Harvard Instruments, USA). Fluorescent images of FITC-dextran were taken using an inverted microscope (Olympus, IX71, Japan) and gradient profiles of FITC-dextran were analyzed using Image J software. FITC-dextran (10 kD molecular weight) was used to balance the molecular weight (12.8 kD) of TGF-β1 (R&D System, USA). Normalized fluorescent intensity profiles of TGF-β1 concentration gradients were obtained from the fluorescent images of FITC-dextran (Fig. 1B).

2.3 A549 human lung alveolar cell culture

A549 human lung alveolar type II epithelial cells were cultured in RPMI1640 medium containing 10% FBS and 1% penicillin-streptomycin. Cells (1.2×10^5 cells/mL) were seeded in 6-well plates and were subsequently cultured overnight. RPMI1640 medium containing 10% FBS and 10 ng/mL TGF-β1 was added into the right inlet reservoir of the microchannel, while RPMI1640 medium without TGF-β1 was placed into the left inlet reservoir.

2.4 Immunocytochemistry

To analyze α-SMA-positive A549 cells exposed to TGF-β1 concentration gradients, the cells were fixed in 4% paraformaldehyde and were subsequently permeabilized with 0.1% Triton X-100 in PBS for 15 min. They were also blocked using 1% BSA in PBS for 30 min at room temperature. The cells were treated with rabbit polyclonal α-SMA antibody (Abcam, USA) at 4°C overnight. After washing with PBS, cells were stained with Alexa Fluor 594 anti-rabbit IgG and DAPI to confirm the cytoskeleton and cell nucleus, respectively.

2.5 Western blot analysis

Cells were lysed by incubation in RIPA buffer (50 mM Tris-Cl pH 7.4, 0.1% NaN_3, 1% Nonidet P-40, 0.25% sodium deoxycholate, 1 mM EDTA, 1 mM Na_3VO_4, 1 mM NaF, and protease inhibitor mixture) for 30 min on ice. A total of 20 μg cell lysate was resolved by SDS-PAGE and transferred to PVDF membranes. Membranes were blocked with 5% nonfat dry milk, probed with E-cadherin (Santa Cruz, CA, USA), vimentin (Sigma Aldrich), and treated with anti-rabbit HRP-conjugated Abs (Cell Signaling Technology, MA, USA) and anti-goat HRP-conjugated Abs (Santa Cruz). The anti-GAPDH Ab (Santa Cruz) was used as a loading control. Immunostained proteins were detected with the ECL detection system (Amersham Pharmacia Biotech, Piscataway, NJ, USA).

3 Results and discussion

3.1 Microfluidic gradient device to culture human lung alveolar epithelial cells

To investigate the effect of cytokine gradients on the behavior of A549 human lung alveolar type II epithelial cells, we developed a microfluidic device that could generate a stable concentration gradient (Fig. 1A). The microfluidic device consisted of the vacuum network and fluidic microchannels containing two inlets and two outlets. The vacuum channel network allowed for reversible bonding between a 6-well plate and the device, as previously described [31, 33]. Fluidic microchannels enabled the generation of a stable concentration gradient in a temporal and spatial manner (Fig. 1B). We observed stable TGF-β1 concentration gradients at a distance of 3.5 mm from the merging point of the two inlet microchannels. To predict the gradient profile in the microfluidic device, we simulated the diffusion of FITC-dextran molecules using FEMLAB software. The Navier–Stokes and diffusion equations were used to simulate the gradient profiles and no-slip boundary conditions were also used for microchannel walls. Computational fluid dynamics represented that the gradient profile of FITC-dextran molecules was closely corresponded to the numerical calculation. A stable gradient profile formed at a distance of 200–700 μm across the microchannel (1 mm in width). The negative (negligible or no TGF-β1) and positive (10 ng/mL TGF-β1) controls were observed at 0–199 μm (bin 1) and 701–1000 μm (bin 7) across the microchannel. The gradient profile (bins 2–6) was equally divided by 5 bins and the interval of each bin was 100 μm. TGF-β1 concentration ranges of bin 2 and bin 3 were 0.6–1.2 and 1.3–3 ng/mL. Bins 4–6 showed 3.1–5.8, 5.9–8.3, and 8.4–9.3 ng/mL TGF-β1 concentrations, respectively. To culture human lung alveolar epithelial cells for 36 h, we constructed extra cylindrical PDMS reservoirs, which contained 500 μL of solution, located at the top of the inlets of the microchannels. Our device enabled the generation of a gradient profile (bins 2–6) with negative (bin 1) and positive (bin 7) controls inside a single chip. This allowed us to examine cellular behavior in response to gradient profiles and flow-based controls so that secreted signaling molecules released from the cells could be removed. Phase contrast images showed that human lung alveolar epithelial cells cultured with TGF-β1 in 6-well plates were elongated into a spindle shape, whereas the cells cultured without TGF-β1 showed a squamous shape (Fig. 2A). When the human lung alveolar epithelial cells exposed to concentration gradients of TGF-β1 were grown in the microfluidic device (Fig. 2B), their morphologies were similar to those in the 6-well plates, despite the fact that they were exposed to the flow-induced shear stress (1.7×10^{-3} dyne/cm^2) in the microfluidic device. This device had a few advantages over previous glass-based microfluidic devices. We initially attempted to culture A549 cells in a glass-based microfluidic device where the fluidic flow was driven by pumping solutions. However, A549 cells failed to firmly adhere on the glass-based microfluidic device, because the pumping mode of syringe pumps pressurized the

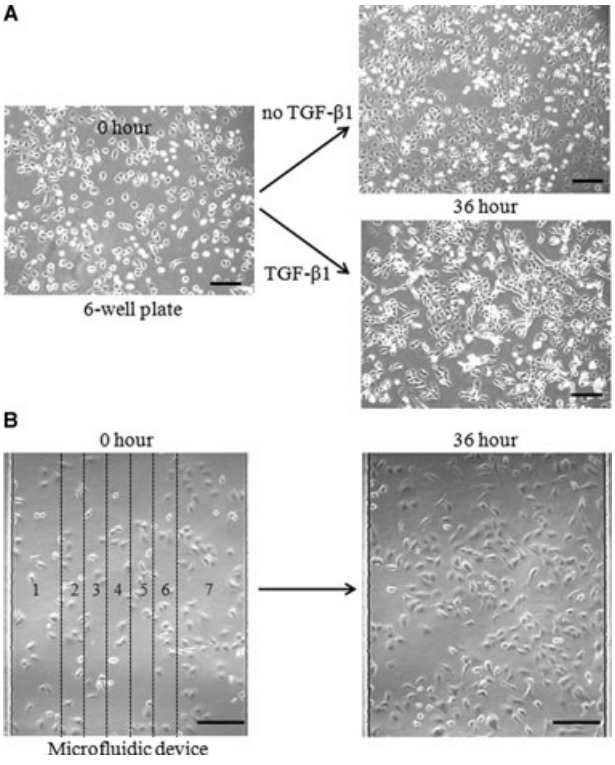

Figure 2. The growth of A549 human lung alveolar epithelial cells cultured in a 6-well plate and the microfluidic device. Phase contrast images of A549 cells that were cultured with or without TGF-β1 in a 6-well plate (A) and the microfluidic gradient device (B). Scale bars are 200 μm.

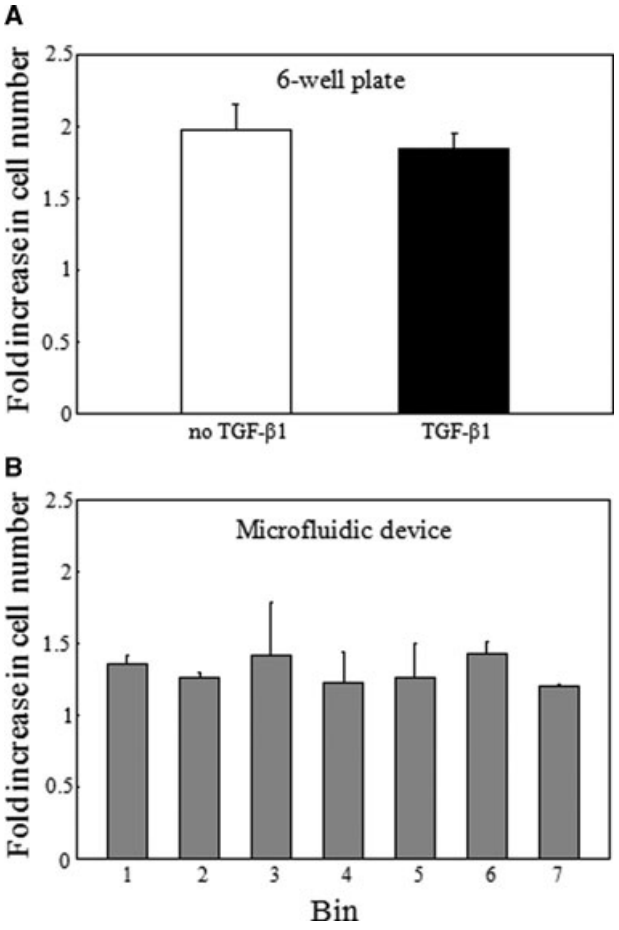

Figure 3. Quantitative analysis of growth of A549 lung alveolar epithelial cells. Proliferation of A549 cells cultured in a 6-well plate (A) and the microfluidic gradient device (B). The fold increase in cell number is expressed as the number of cells grown over 36 h divided by the initial cell number.

microchannels, hindering the cells to adhere on the glass substrate. To circumvent this problem, we used the microfluidic device with negligible shear stress (1.7×10^{-3} dyne/cm^2) driven by a low withdrawal rate (0.15 μL/min), which could provide a favorable environment for the anchorage-dependent cells. In addition, our device was able to be directly mounted on the cells that had been cultured on 6-well plates.

3.2 Growth of human lung alveolar epithelial cells

We measured proliferation of the cells cultured in the microfluidic gradient device and the 6-well plate. We analyzed the growth of human lung alveolar epithelial cells using fold increase in cell number, which was the number of cells cultured for 36 h divided by the initial cell number. For the 6-well plates, we did not observe a significant difference in cell proliferation between TGF-β1 and no TGF-β1 control, showing that there was a 1.7–1.9 fold increase in cell number (Fig. 3A). To quantify the proliferation of human lung alveolar epithelial cells exposed to TGF-β1 gradients in the microfluidic device, we analyzed cell growth in bins 2–6, indicating a 1.3–1.4 fold increase in cell number. The growth of human lung alveolar epithelial cells cultured in the microfluidic gradient device was slightly decreased as compared to the 6-well plate control. The difference appeared to be caused by the shear stress formed in the microfluidic device. There are conflicting reports whether TGF-β1 augments the proliferation of A549 cells. For instance, one report shows proliferation of A549 cells in response to 5 ng/mL or more TGF-β1 [34], whereas another study shows that TGF-β1 (12.5 ng/mL) inhibits proliferation of A549 cells [35]. Although there are conflicting data with regard to the effect of TGF-β1 on proliferation of A549 cells [34, 35], our results support that TGF-β1 has a slightly inhibitory effect on cell growth.

3.3 TGF-β1 gradient-induced EMT response

To investigate the EMT behavior of human lung alveolar epithelial cells cultured in a microfluidic gradient device, the microfluidic gradient device was peeled off the 6-well plate after removing negative pressure. In the 6-well plate, treatment with TGF-β1 led to a significant increase in cells positive to α-SMA, which was an essential component of actin stress fibers and was used as a mesenchymal marker (Fig. 4A). We

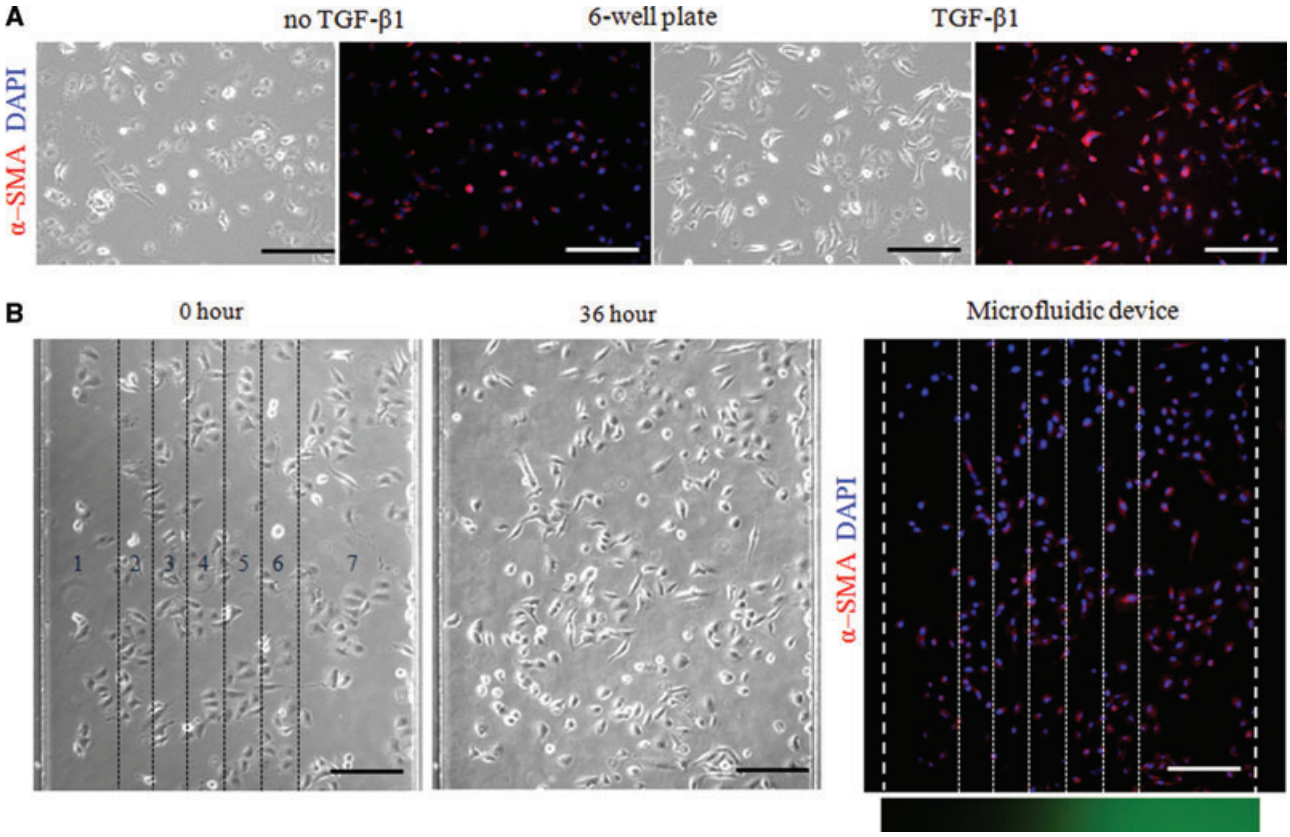

Figure 4. Expression of α-SMA in A549 lung alveolar epithelial cells in response to the TGF-β1 gradient in a 6-well plate (A) and the microfluidic gradient device (B). α-SMA and cell nuclei are indicated in red and blue. Scale bars are 200 μm.

observed the effect of the TGF-β1 concentration gradient on EMT behavior, as determined by the appearance of α-SMA-positive cells depending on TGF-β1 concentrations (Fig. 4B). It showed that α-SMA-positive cells appeared unevenly in the different bins of the microfluidic gradient device and depended on TGF-β1 concentrations, whereas they appeared evenly throughout the 6-well plate cultures. This result indicates that human alveolar epithelial cells cultured in the microfluidic gradient device are able to undergo spindle-shaped fibrosis and an EMT-like fibroblastic phenotype transition in response to TGF-β1, as in plate cultures. To determine the phenotypic change of A549 cells in response to TGF-β1, we measured the longitudinal length and width of the epithelial cells exposed to the TGF-β1 concentration gradients. We measured the cell elongation ratio, defined as the cell longitudinal length divided by cell width. In the 6-well plate, the ratio was 2.3 times greater in cells cultured with TGF-β1 than in those without TGF-β1 (Fig. 5A). To confirm the effect of the TGF-β1 concentration gradient on cell elongation, we also analyzed the ratio of cell elongation in bins in the microfluidic gradient device (Fig. 5B). The quantitative analysis showed that the ratio of cell elongation was linearly proportional to TGF-β1 concentrations, indicating that the cell elongation ratio in bin 2 (0.6–1.2 ng/mL TGF-β1), bin 4 (3.1–5.8 ng/mL TGF-β1), and bin 6 (8.4–9.3 ng/mL TGF-β1) was 1.4, 1.9, and 2.6, respectively. To demonstrate whether biochemical phenotypes correlated with the cellular behavior in response to TGF-β1, three independent Western blottings were carried out with cells from plate cultures (Fig. 5C). The expression of E-cadherin, a cell–cell junction and epithelial marker, was inversely related to TGF-β1 concentration with a concomitant increase in the expression of vimentin, another important mesenchymal marker. A previous report demonstrated EMT phenotypic changes of A549 cells in response to increasing concentrations of TGF-β1 (0.01–10 ng/mL) in 6-well plate cultures [10]. In this study, A549 cells underwent phenotypic changes of EMT only when they were exposed to 1 ng/mL or more TGF-β1, whereas they did not exhibit any sign of EMT responses in response to less than 1 ng/mL TGF-β1 [10]. In our microfluidic device that generated a stable gradient profile, A549 cells exactly sense a particular concentration of TGF-β1 and initiate to respond EMT. Therefore, the microfluidic device is of great benefit to reproduce EMT behavior in a gradient-dependent manner.

A report has previously shown EMT of rat alveolar epithelial type II cells in a microfluidic chamber array with a few attributes including continuous perfusion, low shear stress, and minimized cross-chamber communication [36]. In this study, the microfluidic device was primarily used to evaluate the role of extracellular matrix cues in EMT responses. The results demonstrated that EMT responses were particularly sensitive to extracellular matrix proteins: cells were

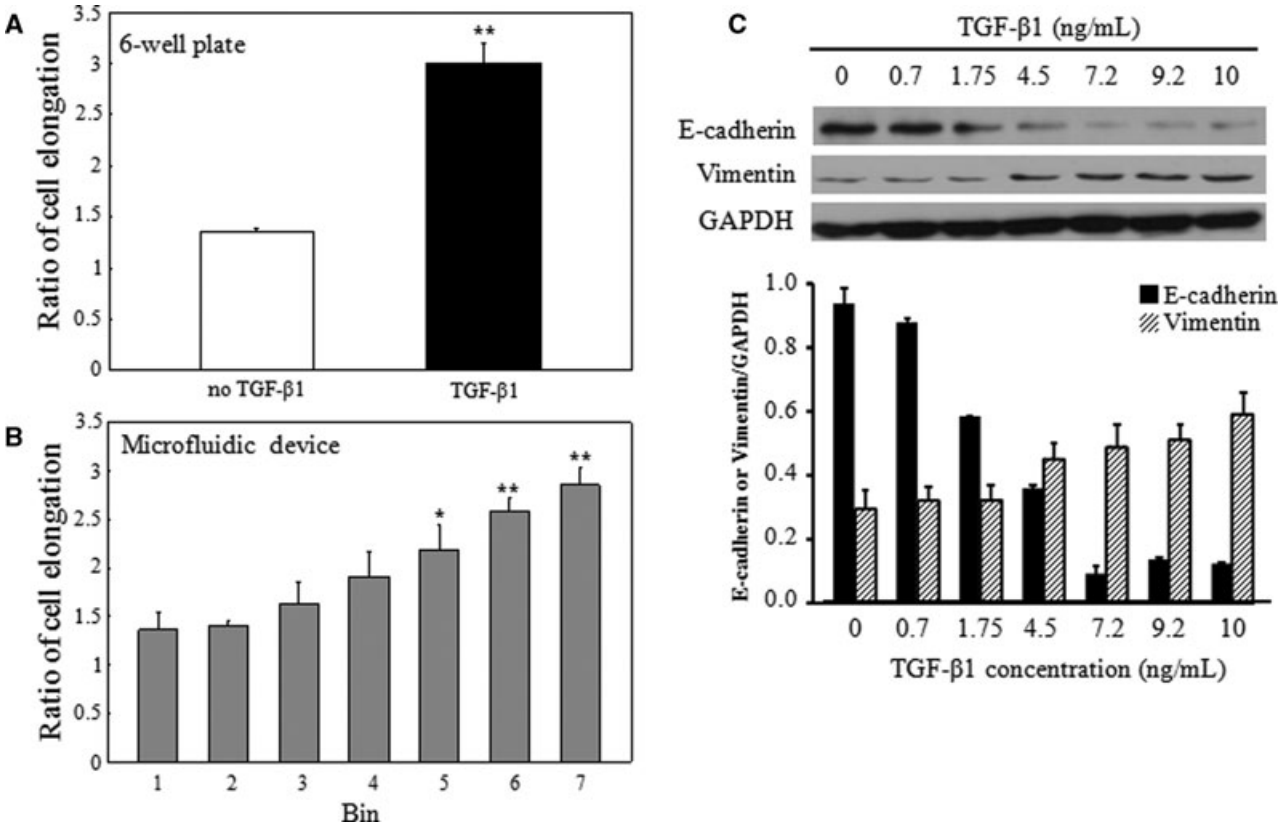

Figure 5. Quantitative analysis of the elongation of A549 human lung alveolar epithelial cells in a 6-well plate (A) and the microfluidic gradient device (B). The cell elongation ratio is the cell longitudinal length divided by cell width (*p <0.05, **p <0.01). (C) Western blot analysis of cells treated with TGF-β1 for 36 h. The blot is probed with anti-E-cadherin and anti-vimentin antibodies. A representative blot is shown in the top with a histogram of the mean ± SEM of three independent experiments in the bottom.

mesenchymal phenotypes in the presence of fibronectin and TGF-β1, while cells cultured on laminin and TGF-β1 developed apoptosis-prone phenotype. Thus, the array is valued as a suitable tool for screening the effect of environment cues on EMT behavior. In our study, we made a microfluidic device with an attribute of gradient profile of TGF-β1. The microfluidic device is of special benefit to determine TGF-β1 concentrations to which the lung epithelial cells respond to initiate and fully undergo EMT. For instance, the cell elongation ratio remained unaltered at bin 2 with TGF-β1 concentrations of 0.6–1.2 ng/mL, as evidenced by no change in cell elongation ratio (Fig. 5B), which was also supported by little change in expression of E-cadherin and vimentin in Western blot analysis (Fig. 5C). The cell elongation ratio began to increase at bin 3 with TGF-β1 concentrations of 1.3–3 ng/mL (Fig. 5B), which was consistent with a decrease in the E-cadherin level (Fig. 5C). At higher TGF-β1 concentrations in compartments including bins 5–7, this microfluidic gradient device sensed a continuum of cellular responses in proportion to TGF-β1 concentration in a quantitative manner, while changes in expression of the biochemical markers were not evident between the bins in the plate cultures. Thus, the microfluidic gradient device allows for analysis of the EMT behavior with a linear correlation to TGF-β1 concentrations as compared with plate cultures. The use of the microfluidic gradient device could be powerful to accurately determine the optimal concentrations of TGF-β1, given that epithelial cells of different tissue origins greatly vary their responses to TGF-β1.

4 Concluding remarks

We developed a microfluidic gradient device to generate a stable TGF-β1 concentration gradient and evaluate EMT in response to TGF-β1. This microfluidic gradient device is of worth for accurately determining the most important parameter for EMT induction, TGF-β1 concentration, at which the lung epithelial cells initiate and fully develop EMT. Therefore, this microfluidic gradient device is applicable for sensing potential stimulants of EMT, such as cigarette smoke in human lung alveolar epithelial cells in a quantitative manner.

This paper was supported by the Science Research Program through the National Research Foundation of Korea (NRF) funded by the Ministry of Education, Science and Technology (Grant Number 2012R1A1A2005822, 20110016331, and

2008–0061860). This work was also supported by Grant A090419 (to I. Y. C.) from the Korea Health 21 R&D Project, Ministry of Health and Welfare, Republic of Korea. S. H. K. and J. H. K. were supported by BK21 from the National Research Foundation. J. M. L. was partially supported by Korea Industrial Technology Foundation (KOTEF) through the Human Resource Training Project for Strategic Technology.

The authors have declared no conflict of interest.

5 References

[1] Kalluri, R., Neilson, E. G., *J. Clin. Invest.* 2003, *112*, 1776–1784.

[2] Zavadil, J., Bottinger, E. P., *Oncogene* 2005, *24*, 5764–5774.

[3] Hay, E. D., *Acta Anat.* 1995, *154*, 8–20.

[4] Roussos, E. T., Keckesova, Z., Haley, J. D., Epstein, D. M., Weinberg, R. A., Condeelis, J. S., *Cancer Res.* 2010, *70*, 7360–7364.

[5] Onder, T. T., Gupta, P. B., Mani, S. A., Yang, J., Lander, E. S., Weinberg, R. A., *Cancer Res.* 2008, *68*, 3645–3654.

[6] Vanderburg, C. R., Hay, E. D., *Acta Anat.* 1996, *157*, 87–104.

[7] Sime, P. J., O'Reilly, K. M., *Clin. Immunol.* 2001, *99*, 308–319.

[8] Willis, B. C., Borok, Z., *Am. J. Physiol. Lung Cell Mol. Physiol.* 2007, *293*, L525–L534.

[9] Liu, Y., Gao, W., Zhang, D., *Clin. Exp. Med.* 2010, *10*, 159–167.

[10] Kasai, H., Allen, J. T., Mason, R. M., Kamimura, T., Zhang, Z., *Respir. Res.* 2005, *6*, 56.

[11] Willis, B. C., Liebler, J. M., Luby-Phelps, K., Nicholson, A. G., Crandall, E. D., du Bois, R. M., Borok, Z., *Am. J. Pathol.* 2005, *166*, 1321–1332.

[12] Kim, K. K., Kugler, M. C., Wolters, P. J., Robillard, L., Galvez, M. G., Brumwell, A. N., Sheppard, D., Chapman, H. A., *Proc. Natl. Acad. Sci. USA* 2006, *103*, 13180–13185.

[13] Chung, B. G., Choo, J., *Electrophoresis* 2010, *31*, 3014–3027.

[14] Keenan, T. M., Folch, A., *Lab. Chip.* 2008, *8*, 34–57.

[15] Whitesides, G. M., *Nature* 2006, *442*, 368–373.

[16] Saadi, W., Wang, S. J., Lin, F., Jeon, N. L., *Biomed. Microdevices* 2006, *8*, 109–118.

[17] Lin, F., Nguyen, C. M., Wang, S. J., Saadi, W., Gross, S. P., Jeon, N. L., *Biochem. Biophys. Res. Commun.* 2004, *319*, 576–581.

[18] Frevert, C. W., Boggy, G., Keenan, T. M., Folch, A., *Lab. Chip.* 2006, *6*, 849–856.

[19] Keenan, T. M., Frevert, C. W., Wu, A., Wong, V., Folch, A., *Lab. Chip.* 2010, *10*, 116–122.

[20] Li Jeon, N., Baskaran, H., Dertinger, S. K., Whitesides, G. M., Van de Water, L., Toner, M., *Nat. Biotechnol.* 2002, *20*, 826–830.

[21] Torisawa, Y. S., Mosadegh, B., Bersano-Begey, T., Steele, J. M., Luker, K. E., Luker, G. D., Takayama, S., *Integr. Biol.* 2010, *2*, 680–686.

[22] Berthier, E., Surfus, J., Verbsky, J., Huttenlocher, A., Beebe, D., *Integr. Biol.* 2010, *2*, 630–638.

[23] Irimia, D., Balazsi, G., Agrawal, N., Toner, M., *Biophys. J.* 2009, *96*, 3897–3916.

[24] Lin, F., Baldessari, F., Gyenge, C. C., Sato, T., Chambers, R. D., Santiago, J. G., Butcher, E. C., *J. Immunol.* 2008, *181*, 2465–2471.

[25] Li, J., Nandagopal, S., Wu, D., Romanuik, S. F., Paul, K., Thomson, D. J., Lin, F., *Lab. Chip.* 2011, *11*, 1298–1304.

[26] Polacheck, W. J., Charest, J. L., Kamm, R. D., *Proc. Natl. Acad. Sci. USA* 2011, *108*, 11115–11120.

[27] Park, J. Y., Yoo, S. J., Hwang, C. M., Lee, S. H., *Lab. Chip.* 2009, *9*, 2194–2202.

[28] Dertinger, S. K., Jiang, X., Li, Z., Murthy, V. N., Whitesides, G. M., *Proc. Natl. Acad. Sci. USA* 2002, *99*, 12542–12547.

[29] Du, Y. N., Hancock, M. J., He, J. K., Villa-Uribe, J. L., Wang, B., Cropek, D. M., Khademhosseini, A., *Biomaterials* 2010, *31*, 2686–2694.

[30] Cimetta, E., Cannizzaro, C., James, R., Biechele, T., Moon, R. T., Elvassore, N., Vunjak-Novakovic, G., *Lab. Chip.* 2010, *10*, 3277–3283.

[31] Kim, S. H., Kang, J. H., Chung, I. Y., Chung, B. G., *Electrophoresis* 2011, *32*, 254–260.

[32] Chung, B. G., Flanagan, L. A., Rhee, S. W., Schwartz, P. H., Lee, A. P., Monuki, E. S., Jeon, N. L., *Lab. Chip.* 2005, *5*, 401–406.

[33] Chung, B. G., Park, J. W., Hu, J. S., Huang, C., Monuki, E. S., Jeon, N. L., *BMC Biotechnol.* 2007, *7*, 60.

[34] Zheng, J., Guan, S., Xu, Q., Liu, J., Song, P., *Chin. Med. J.* 2012, *125*, 2734–2740.

[35] Halder, S. K., Beauchamp, R. D., Datta, P. K., *Neoplasia* 2005, *7*, 509–521.

[36] Park, E. S., Brown, A. C., DiFeo, M. A., Barker, T. H., Lu, H., *Lab. Chip.* 2010, *10*, 571–580.

